⌘ *Author's Choice*

THE JOURNAL OF BIOLOGICAL CHEMISTRY VOL. 287, NO. 42, pp. 35658–35668, October 12, 2012
© 2012 by The American Society for Biochemistry and Molecular Biology, Inc. Published in the U.S.A.

Glycosylation Is Dispensable for Sorting of Synaptotagmin 1 but Is Critical for Targeting of SV2 and Synaptophysin to Recycling Synaptic Vesicles*

Received for publication, July 6, 2012, and in revised form, August 6, 2012 Published, JBC Papers in Press, August 20, 2012, DOI 10.1074/jbc.M112.398883

Sung E. Kwon[1] **and Edwin R. Chapman**[2]

From the Howard Hughes Medical Institute, Department of Neuroscience, University of Wisconsin, Madison, Wisconsin 53706

Background: Whether glycosylation is essential for targeting of synaptic vesicle proteins is unclear.
Results: Glycosylation-deficient synaptotagmin 1 is correctly targeted and functions normally whereas trafficking of SV2 and synaptophysin is severely affected by the loss of glycosylation.
Conclusion: Glycosylation is of differential importance for different synaptic vesicle proteins.
Significance: This represents the first quantitative comparison of the trafficking of wild-type and mutant synaptic vesicle glycoproteins.

Glycosylation is a major form of post-translational modification of synaptic vesicle membrane proteins. For example, the three major synaptic vesicle glycoproteins, synaptotagmin 1, synaptophysin, and SV2, represent ~30% of the total copy number of vesicle proteins. Previous studies suggested that glycosylation is required for the vesicular targeting of synaptotagmin 1, but the role of glycosylation of synaptophysin and SV2 has not been explored in detail. In this study, we analyzed all glycosylation sites on synaptotagmin 1, synaptophysin, and SV2A via mutagenesis and optical imaging of pHluorin-tagged proteins in cultured neurons from knock-out mice lacking each protein. Surprisingly, these experiments revealed that glycosylation is completely dispensable for the sorting of synaptotagmin 1 to SVs whereas the *N*-glycans on SV2A are only partially dispensable. In contrast, *N*-glycan addition is essential for the synaptic localization and function of synaptophysin. Thus, glycosylation plays distinct roles in the trafficking of each of the three major synaptic vesicle glycoproteins.

Synaptic vesicles (SVs)[3] harbor a specific set of membrane proteins, so precise sorting mechanisms underlie their biogenesis and recycling in nerve terminals (1). The sorting process may occur at several different levels along the SV biogenesis pathway. Axonal (*i.e.* SV) *versus* dendritic proteins might be organized into different microdomains at the trans-Golgi network and inserted into distinct sets of transport vesicles (1, 2). Alternatively, SV proteins might distribute to the surface of both axons and dendrites, followed by selective endocytosis from dendritic membranes (3). In general, little is known concerning SV biogenesis or how SV components are specifically sorted.

Glycosylation is a major post-translational modification that affects folding, sorting, and trafficking of a number of proteins (4–6). *N*-Glycosylation involves the attachment of oligosaccharides to asparagine residues of a target protein during polypeptide synthesis in the endoplasmic reticulum (ER). *N*-Glycosylation plays a role in apical/basolateral sorting in polarized epithelial cells (6). *O*-Glycosylation involves addition of glycans to serine or threonine residues in the Golgi and can act as an additional sorting signal (7).

SVs contain three major glycoproteins, synaptotagmin 1 (syt1), SV2, and synaptophysin (syp), collectively representing ~30%, by copy number, of the total complement of SV proteins (8). The function of the carbohydrates on these proteins remains unclear. Syt1 is a Ca^{2+} sensor for synchronous neurotransmitter release (9, 10). *N*-Glycosylation was reported to be essential for the vesicular targeting of syt1 in neuroendocrine cells, which, however, are devoid of recycling SVs (11). In another study, *O*-glycosylation appeared to be important for the vesicular sorting of syt1 in neuroendocrine cells (12). At present, whether glycosylation is essential for localization of syt1 to SVs remains an open question.

SV2 is a 12-transmembrane domain glycoprotein of unknown function. There are three isoforms, A, B, and C, with SV2A being the most widely expressed in the brain (13). Substitution of all three glycosylation sites of SV2A led to reduced expression and accumulation of the protein in the cell body of neurons (14–16). The single point mutations had no obvious effects, but whether these mutants sort to recycling SVs was not tested.

Syp is a 4-transmembrane domain glycoprotein that regulates the kinetics of SV endocytosis (17, 18). When expressed in human hepatoma cells, wild type, as well as a nonglycosylated mutant form of syp, sorted to small translucent vesicles that resemble SVs (19). These findings suggest that glycosylation might be dispensable for trafficking of syp, but this idea has not been tested in neurons.

* This study was supported, in whole or in part, by National Institutes of Health Grant MH 61876.
⌘ *Author's Choice*—Final version full access.
[1] Supported by an Epilepsy Foundation predoctoral fellowship.
[2] To whom correspondence should be addressed: 1300 University Ave., SMI 203, Madison, WI 53706. Tel.: 608-263-1762; E-mail: chapman@wisc.edu.
[3] The abbreviations used are: SV, synaptic vesicle; ER, endoplasmic reticulum; syt1, synaptotagmin 1; syp, synaptophysin.

Here we examined the role of glycosylation in the sorting of syt1, SV2A, and syp to recycling SVs and observed that the functional importance of glycosylation varies dramatically among different SV proteins.

EXPERIMENTAL PROCEDURES

Antibodies and Mouse Lines—Anti-syp (7.2) and anti-syntaxin (HPC-1) mouse monoclonal antibodies were generously provided by R. Jahn (Gottingen, Germany). An anti-SV2A mouse monoclonal antibody was purchased from Synaptic Systems (Gottingen, Germany). Rabbit anti-GFP and all secondary antibodies were purchased from Abcam (Cambridge, MA). The syt1 knock-out (KO) mouse line was obtained from Jackson Laboratory (Bar Harbor, ME) (10), the syp KO mouse line was kindly provided by R. Leube (Mainz, Germany) (20), and the SV2A/B KO mouse line was kindly provided by R. Janz (Houston, TX) (21). Mouse lines were maintained as heterozygous breeding pairs.

Molecular Biology—Syt1-pH and sypHy constructs were kindly provided by T. A. Ryan (New York, NY) and L. Lagnado (Cambridge, United Kingdom), respectively (22, 23). SV2A-pH was described previously (18). Syt1-pH constructs were delivered into neurons either by calcium phosphate-mediated transfection (all experiments in Figs. 1 and 2 except for the Western blot analysis in Fig. 1*B*) or by lentiviral infection (Figs. 1*B* and 3). The transfected syt1-pH constructs were based on a mammalian expression vector, pCI (Promega; Madison, WI), that contains the human cytomegalovirus promoter (22, 24). SypHy and SV2A-pH constructs were delivered into neurons only by lentiviral infection. Syt1-pH, sypHy, and SV2A-pH were subcloned into the pLox Syn-DsRed-Syn-GFP lentiviral vector (pLox) (kindly provided by F. Gomez-Scholl (Seville, Spain)) by substituting the DsRed coding sequence with the indicated pHluorin-fusion construct. GFP in the pLox vector was replaced by mCherry to avoid spectral overlap with pHluorin. One synapsin promoter directs the expression of mCherry whereas the other drives the expression of the indicated pHluorin construct. Mutant proteins that lack glycosylation sites were generated using a QuikChange II XL kit (Stratagene, La Jolla, CA).

Neuronal Cultures and Viruses—Primary hippocampal cultures from mice were prepared as described previously in accordance with the guidelines of the National Institutes of Health, as approved by the Animal Care and Use Committee of the University of Wisconsin-Madison (25). Briefly, hippocampi from post-natal mice (0–1 day after birth) of either sex were dissociated in 0.25% trypsin, washed twice in Hanks' Buffered Salt Solution, and plated onto poly-D-lysine)-coated 15-mm coverslips. Neurons were transfected using calcium phosphate on *in vitro* day 7 or infected with lentiviruses on *in vitro* day 5 and subjected to experiments between *in vitro* day 14 and 20. For transfection, we followed closely a published protocol (26). Briefly, 50 μl of transfection mixture was prepared by gently adding 25 μl of 250 mM $CaCl_2$ solution containing 1 μg of plasmid DNA to 25 μl of 2× HEPES-buffered saline (Clontech). Precipitates were allowed to form for 20 min at room temperature, and the 50-μl mixture was added to neurons on each coverslip in a 24-well plate. Lentiviruses were generated using human embryonic kidney 293T cells as described previously (27).

Live Cell Imaging—Neurons were continuously perfused with bath solution (140 mM NaCl, 5 mM KCl, 2 mM $CaCl_2$, 2 mM $MgCl_2$, 10 mM HEPES, 10 mM glucose, 50 μM D-AP5, and 10 μM CNQX adjusted to 310 mosM with glucose, pH 7.4) at room temperature during imaging. For field stimulation, 1-ms constant voltage pulses (70 V) were delivered digitally using ClampEX 10.0 software via two parallel platinum wires spaced by 10 mm in the imaging chamber (Warner Instruments; Hamden, CT). For the low pH/NH_4Cl perfusion experiments, the low pH solution was prepared by replacing HEPES in the bath solution with MES (pK_a 6.1), and the pH was adjusted to 5.5. Solution exchange was driven by an MPS-2 multi-channel perfusion system (World Precision Instruments; Sarasota, FL). Time-lapse images, taken at 1-s intervals, were obtained using an inverted microscope (Nikon TE300) with a 100× 1.40 numerical aperture oil objective under illumination with a xenon light source controlled by a rapid wavelength switcher (Lambda DG-4). Fluorescence changes at individual boutons were detected using a Cascade 512II EMCCD camera (Roper Scientific; Berlin, Germany) with 2 × 2 binning; data were collected and analyzed off-line using MetaMorph 6.0 software.

Immunocytochemistry and Western Blot Analysis—Neurons on coverslips were washed in PBS, fixed with 4% paraformaldehyde for 10 min, and permeabilized in PBS with 0.25% Triton X-100. After three washes, neurons were incubated for 20 min in antibody buffer (PBS with 10% goat serum, 0.1% Triton X-100). Primary antibodies were prepared in fresh antibody buffer and incubated overnight at 4 °C. Neurons were washed and incubated with secondary antibody for 30 min at room temperature, washed in PBS, mounted onto slides, and imaged using an Olympus FV1000 confocal microscope with a 60× 1.10 numerical aperture water immersion objective.

Images were acquired with identical laser and gain settings, and the threshold was determined separately for each channel to include all boutons with diameters between 3 and 7 pixels (0.7 ~ 1.6 μm). The percent of total thresholded area of pHluorin staining that overlapped with the thresholded area of a SV marker (synaptophysin or SV2A) was calculated using MetaMorph (28). Results were pooled from four coverslips from two independent cultures.

Neuronal cell lysates were prepared from virus-infected neurons as described previously (15). Briefly, 100 μl of ice-cold lysis buffer (PBS containing 1% Triton X-100, 0.05% SDS, and a protease inhibitor mixture) was added to each coverslip in a 24-well plate. Lysates were harvested on ice, incubated for 5 min at 4 °C, and centrifuged at 16,000 × *g* for 25 min. Supernatants were subjected to SDS-PAGE and Western blot analysis.

RESULTS

Lack of N- or O-Glycosylation Does Not Affect Vesicular Sorting of Syt1 in Knock-out Neurons, but Does Affect Sorting in Wild-type Neurons—Previous studies reported that *N*-glycosylation is essential for vesicular targeting of syt1 in PC12 cells and SV targeting in neurons (11, 29). We tested this claim in

neurons using the pHluorin-tagged protein (syt1-pH) (22, 24). Syt1 has one *N*-glycosylation site (Asn-24) within its luminal domain, which was mutated to Gln (Q) (Fig. 1*A*). We reported previously, using the lentivirus system that is also employed here, that wild-type (WT) syt1 is expressed at a level that is similar to the endogenous protein (30). We compared the levels of WT and the N24Q mutant syt1-pH proteins, expressed in syt1 KO neurons, by immunoblot analysis using an antibody directed against GFP; similar levels of expression were observed (Fig. 1*B*). To test whether WT and the N24Q mutant are sorted to SVs, we transfected these constructs into WT neurons and compared the recycling kinetics. WT neurons expressing WT or N24Q syt1-pH were depolarized using a 20-Hz, 5-s stimulus train (Fig. 1*C*). Time-lapse images with 1-s intervals were acquired 10 s prior to the beginning of stimulus train and up to 100 s after the train. The decay phase of individual fluorescence traces was fitted with single exponential functions to determine the post-stimulus endocytic time constant. This time constant was not significantly different between WT and N24Q syt1-pH proteins, showing that the N24Q mutation does not affect recycling of syt1 (Fig. 1*D*, *left panel*).

To determine the steady-state distribution of syt1 on vesicles *versus* the plasma membrane, we superfused neurons with low pH buffer (pH 5.5) and then NH_4Cl solution (Fig. 1*C*). The low pH buffer quenches the fluorescence of syt1-pH on the cell surface, causing a reduction in fluorescence (F_1) that corresponds to the surface fraction (Figs. 1*C* and 3*F*). The ammonia in the NH_4Cl solution alkalinizes the acidic lumen of SVs and dequenches syt1-pH, leading to a rapid rise in fluorescence (F_2), which reveals the internal pool within acidic organelles (Figs. 1*C* and 3*F*). The fraction of syt1-pH on the plasma membrane surface was estimated as $F_1/(F_1 + F_2)$ (see Fig. 3, *F* and *G*). We plotted the fraction of syt1-pH on the plasma membrane surface *versus* the magnitude of evoked fluorescence increases in response to a stimulus train (20 Hz, 5 s) for individual boutons (Fig. 1, *D* and *E*; *middle panels*). In WT neurons, the N24Q syt1-pH exhibited greater accumulation on the plasma membrane (WT: 0.35 ± 0.1, N24Q: 0.51 ± 0.3) and smaller fluorescence changes following the stimulus train (20 Hz, 5 s) as compared with the WT syt1-pH; boutons expressing WT syt1-pH were clearly separable from those expressing N24Q syt1-pH (Fig. 1*D*, *middle* and *right panels*). N24Q mutation led to an increase in the surface fraction of syt1-pH and a concomitant reduction of the protein fraction targeted to recycling vesicles. This observation is somewhat reminiscent of the result obtained using PC12 cells in which N24Q mutant syt1 was reported to be localized to the plasma membrane rather than vesicular membrane; however, in that study incorporation of syt1 into the plasma membrane was not directly demonstrated. Moreover, in our experiments, the increase in the amount of syt1 accumulation at the cell surface was limited (from ~35% to ~50%).

We determined whether the presence of endogenous syt1, as in WT neurons, would influence the vesicular sorting of N24Q mutant syt1. To this end, WT or N24Q syt1-pH was expressed in syt1 KO neurons, and the same experiments described above were carried out. The post-stimulus endocytic time course was not significantly different between WT and N24Q syt1-pH proteins, suggesting that the N24Q mutation does not affect internalization of the cargo regardless of the endogenous syt1 level (Fig. 1*E*). Interestingly, the two populations of boutons expressing either WT or N24Q syt1-pH were indistinguishable in terms of the surface fraction (WT: 0.18 ± 0.08, N24Q: 0.19 ± 0.07) or the magnitude of evoked fluorescence change (Fig. 1*E*, *middle* and *right panels*). Therefore, the putative role of glycosylation for vesicular targeting of syt1 becomes manifest only in the presence of endogenous syt1; in the absence of endogenous syt1, the N24Q mutant syt1 sorts and recycles normally.

A previous study in PC12 cells suggested that *O*-glycosylation, instead of *N*-glycosylation, is important for vesicular sorting of syt1 (12). To test the importance of *O*-glycosylation, we expressed T15,16A mutant syt1-pH in which the two *O*-glycosylated Thr residues were substituted by Ala, in WT or syt1 KO neurons. We determined the total pHluorin fluorescence per bouton by NH_4Cl superfusion and found that it was not different between WT and the T15,16A mutant expressed in syt1 KO neurons; *O*-glycosylation did not affect the expression level of syt1 (Fig. 2*B*).

We monitored the retrieval kinetics following the stimulus train (20 Hz, 5 s), and we again measured the steady-state distribution of the WT and mutant proteins. The endocytic time course was not altered by the T15,16A mutation either in WT or syt1 KO neurons (Fig. 2, *C* and *D*, *left panels*). Similar to the N24Q mutant, T15,16A syt1-pH exhibited an increased plasma membrane fraction (WT: 0.35 ± 0.1; T15,16A: 0.56 ± 0.1) and reduction of evoked fluorescence in WT, but not in syt1 KO neurons (Fig. 2, *C* and *D*, *middle* and *right panels*).

These results from *N*- or *O*-glycosylation mutants suggest that endogenous and exogenous syt1 proteins might compete for a limited number of slots on SVs during biogenesis. In the presence of endogenous syt1, as in WT neurons, the mutant syt1 lacking *N*- or *O*-glycans might be less competent for occupying those slots than endogenous WT syt1, leading to enhanced accumulation of the protein on the plasma membrane. In the absence of endogenous syt1, as in KO neurons, there is no competition such that the glycan-deficient form would be as competent as WT syt1-pH for occupying putative slots on SVs.

Glycosylation Is Not Required for the Sorting of Syt1 to Cycling SVs—Removing all glycosylation sites of syt1 might uncover alterations in the subcellular localization of the protein that were not apparent in the experiments described in which we examined *N*- and *O*- glycosylation independently. We therefore created a T15,16A/N24Q mutant form of syt1-pH in which the two *O*-glycosylation sites (Thr-15, Thr-16) and the *N*-glycosylation site (Asn-24) were mutated to Ala (A) and Gln (Q), respectively (Fig. 3*A*). Because these mutations result in a larger alteration in syt1 (*i.e.* the complete absence of glycan), we confirmed the synaptic localization of the mutant protein after expression in syt1 (KO) neurons using lentivirus; WT syt1 served as a control. A high degree of co-localization with synapsin was observed for both the WT and mutant proteins (Fig. 3, *B* and *C*).

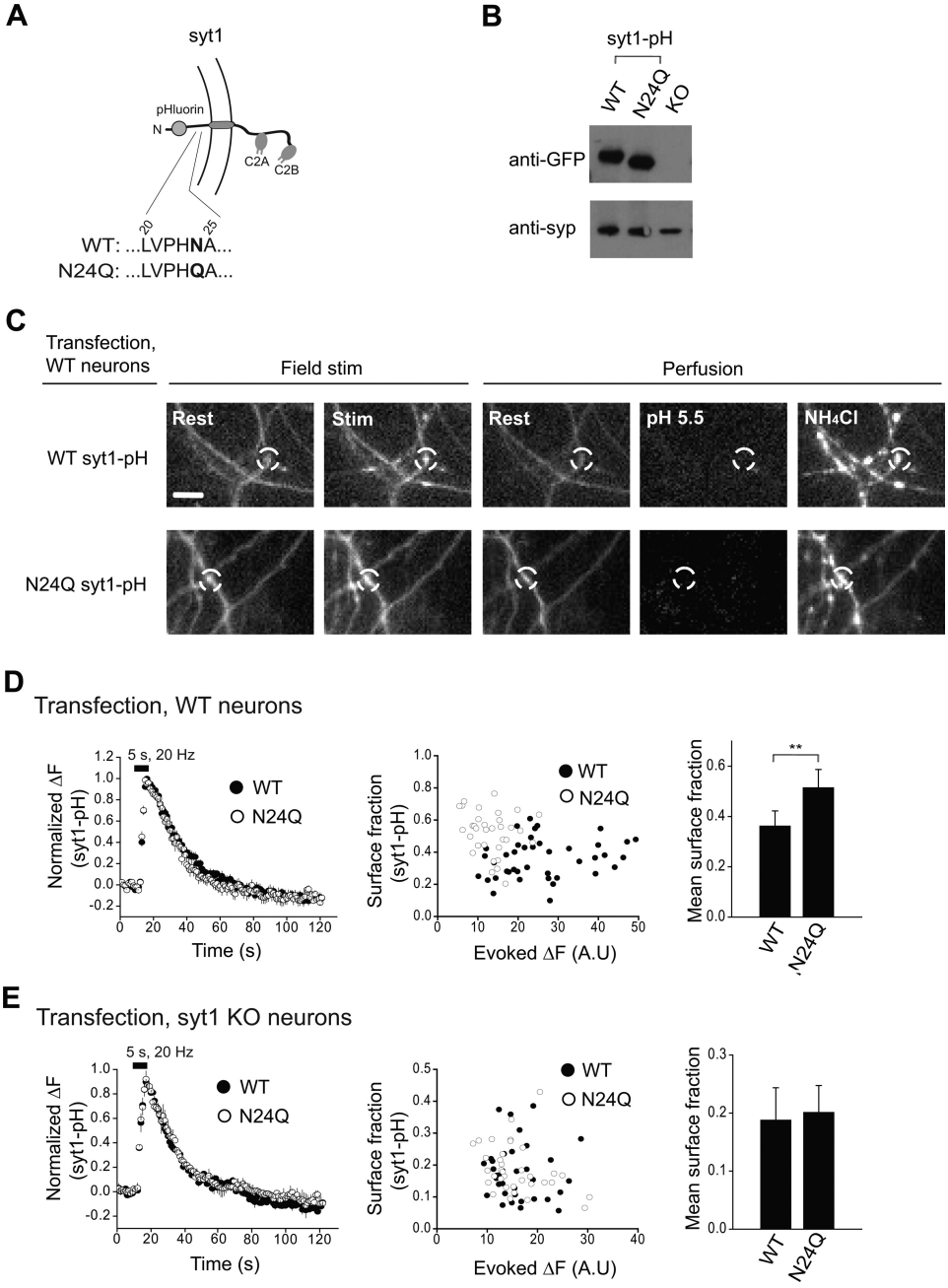

FIGURE 1. **Loss of the *N*-glycan has differential effects on the localization of syt1-pH in WT *versus* syt1 KO neurons.** *A*, schematic diagram shows the *N*-glycosylated Asn residue (*N*) in the luminal domain of WT syt1. N24Q denotes substitution of Asn with a Gln residue. *B*, Western blot shows expression levels of WT and N24Q mutant forms of syt1-pH. Samples were prepared from syt1 KO neurons infected with lentivirus. Anti-GFP antibody was used to detect the pHluorin. Syp served as a loading control. *C*, *top*, representative images from WT neurons in which syt1-pH was expressed by calcium phosphate-mediated transfection are shown. The *first two panels* show presynaptic boutons before and after stimulation at 20 Hz for 5 s. The *next three panels* show the same set of boutons during perfusion with low pH buffer followed by the NH_4Cl solution. The surface fluorescence signals were quenched by applying low pH solution. Internal acidic fluorescence signals were subsequently dequenched by NH_4Cl perfusion. The surface fraction of syt1-pH was determined as detailed in the legend to Fig. 3, *F* and *G*. *Bottom*, same experiment described in the *top panel* was repeated using N24Q syt1-pH. *Scale bar*, 2 μm. *D*, *left*, average normalized fluorescence traces for WT (*closed circles*) and N24Q mutant forms (*open circles*) of syt1-pH in response to the 20-Hz, 5-s stimulus train are shown. Average is from four coverslips, 25 boutons each. Each coverslip represents an independent neuronal culture. *Middle*, surface fraction of syt1-pH was plotted against the evoked fluorescence change for individual presynaptic boutons in transfected WT neurons. Each *circle* represents a bouton expressing WT (*closed circles*, 40 boutons from two coverslips) or N24Q (*open circles*, 34 boutons from two coverslips) syt1-pH. The two groups show clear segregation. *Right*, comparison of mean surface fraction between WT and N24Q mutant forms of syt1-pH expressed in WT neurons is shown. Average is from four coverslips, 25 boutons each. *E*, same experiments described above in *C* and *D* were repeated in syt1 KO neurons. *Left*, average normalized fluorescence traces for WT (*closed circles*) and N24Q mutant forms (*open circles*) of syt1-pH in response to the 20-Hz, 5-s stimulus train are shown. Average is from four coverslips, 25 boutons each. *Middle*, surface fraction of syt1-pH was plotted against the evoked fluorescence change for individual boutons in syt1 KO neurons expressing WT (*closed circles*, 33 boutons from two coverslips) or N24Q (*open circles*, 33 boutons from two coverslips) syt1-pH. No segregation was observed between the two groups. *Right*, comparison of mean surface fraction between WT and N24Q mutant syt1-pH expressed in KO neurons is shown. Average is from four coverslips, 25 boutons each. To assess significance, Student's *t* test was used throughout this study. **, $p < 0.01$. *Error bars*, S.E.

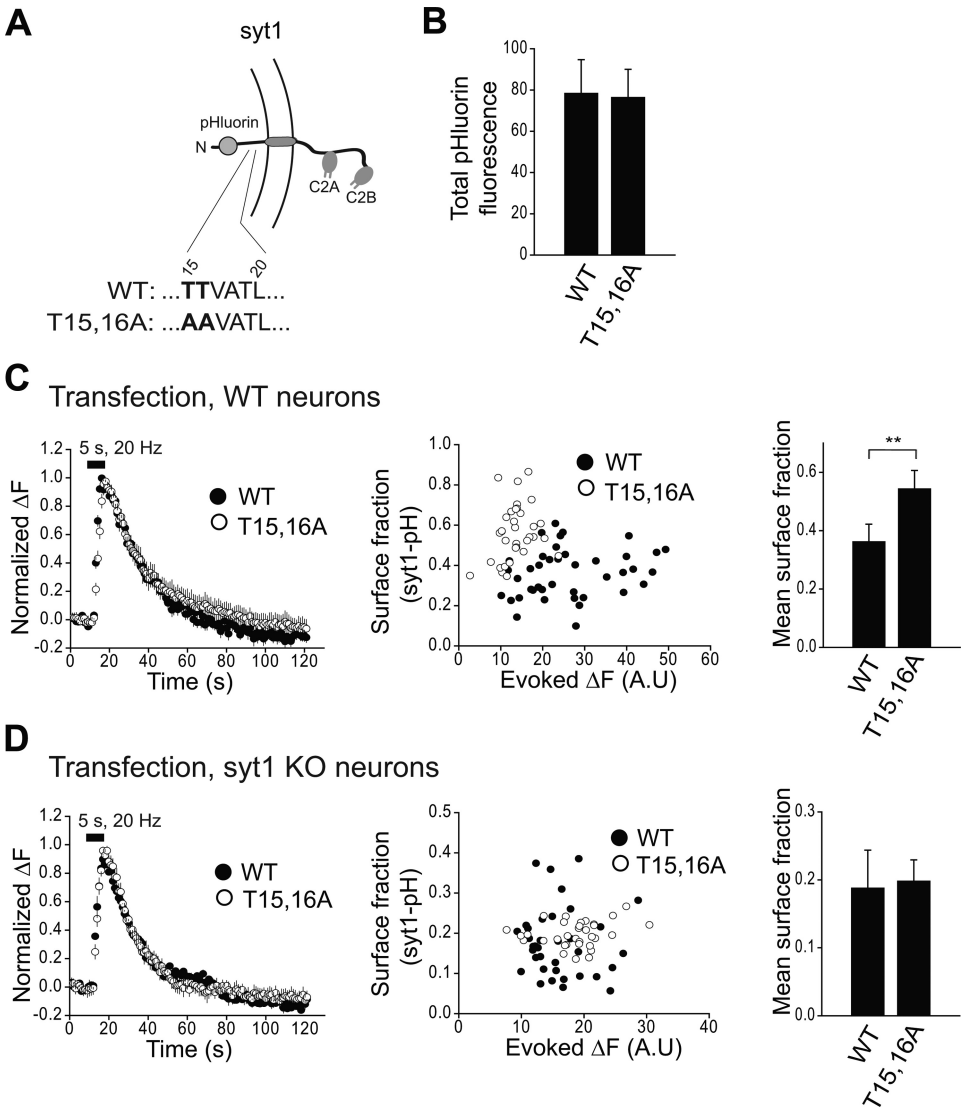

FIGURE 2. **Loss of the *O*-glycan has differential effects on the localization of syt1-pH in WT *versus* syt1 KO neurons.** *A*, schematic diagram shows *O*-glycosylated Thr residues in WT syt1. T15,16A denotes substitution of Thr-15 and Thr-16 with Ala residues. *B*, expression levels of WT and the T15,16A mutant syt1-pH were compared by determining total pHluorin fluorescence per bouton in arbitrary units by NH_4Cl superfusion (as shown in the legend of Fig. 1*C*) of syt1 KO neurons transfected with these constructs. *C*, *left*, average normalized fluorescence traces for WT (*closed circles*) and T15,16A mutant forms (*open circles*) of syt1-pH, which were expressed in WT neurons by calcium phosphate-mediated transfection, in response to the 20-Hz, 5-s stimulus train are shown. Average is from four coverslips, 25 boutons each. *Middle*, surface fraction of syt1-pH was plotted against the evoked fluorescence change for individual presynaptic boutons in transfected WT neurons. Each *circle* represents a bouton expressing WT (*closed circles*, 40 boutons from two coverslips) or T15,16A (*open circles*, 32 boutons from two coverslips) syt1-pH. The two groups show clear segregation. *Right*, comparison of mean surface fraction between WT and T15,16A mutant syt1-pH is shown. Average is from four coverslips, 25 boutons each. *D*, same experiment described in *C* was repeated in syt1 KO neurons. *Left*, average normalized fluorescence traces for WT (*closed circles*) and T15,16A mutant forms (*open circles*) of syt1-pH in response to the 20-Hz, 5-s stimulus train are shown. Average is from four coverslips, 20 boutons each. *Middle*, surface fraction of syt1-pH was plotted against the evoked fluorescence change for individual boutons in syt1 KO neurons expressing WT (*closed circles*, 33 boutons from two coverslips) or T15,16A (*open circles*, 32 boutons from two coverslips) mutant syt1-pH. No segregation was observed between the two groups. *Right*, comparison of mean surface fraction between WT and the T15,16A mutant syt1-pH is shown. **, $p < 0.01$. *Error bars*, S.E.

We then analyzed the recycling kinetics and the surface fraction of nonglycosylated syt1-pH (Fig. 3, *D* and *E*), using a stronger stimulus train (10 Hz, 30 s) than utilized above. Neurons were also superfused with low pH buffer (pH 5.5) and then the NH_4Cl solution (Fig. 3*F*). The endocytic time constant was not significantly different between WT (18.5 ± 0.8 s) and the T15,16A/N24Q mutant syt1-pH (19.2 ± 0.8 s) (Fig. 3*E*). The fluorescence change evoked by the stimulus train (10 Hz, 30 s) was normalized to the maximal fluorescence change during NH_4Cl superfusion. This fraction was used as an empirical measurement of the recycling pool size, which was not significantly different between WT (0.25 ± 0.08) and the T15,16A/N24Q mutant (0.26 ± 0.08) (Fig. 3*G*). The surface fraction, estimated as $F_1/(F_1 + F_2)$, was also not altered in the T15,16A/N24Q mutant (WT: 0.12 ± 0.02; T15,16A/N24Q: 0.11 ± 0.02) (Fig. 3, *F* and *H*).

Although these results indicate that glycosylation of syt1 is not important for the recycling of the protein, it might play a role in recycling of SVs. We therefore examined whether mutant syt1, lacking all glycans, could rescue the slow SV endocytosis phenotype in syt1 KO neurons by expressing untagged, T15,16A/N24Q syt1 in syt1 KO neurons and monitoring SV

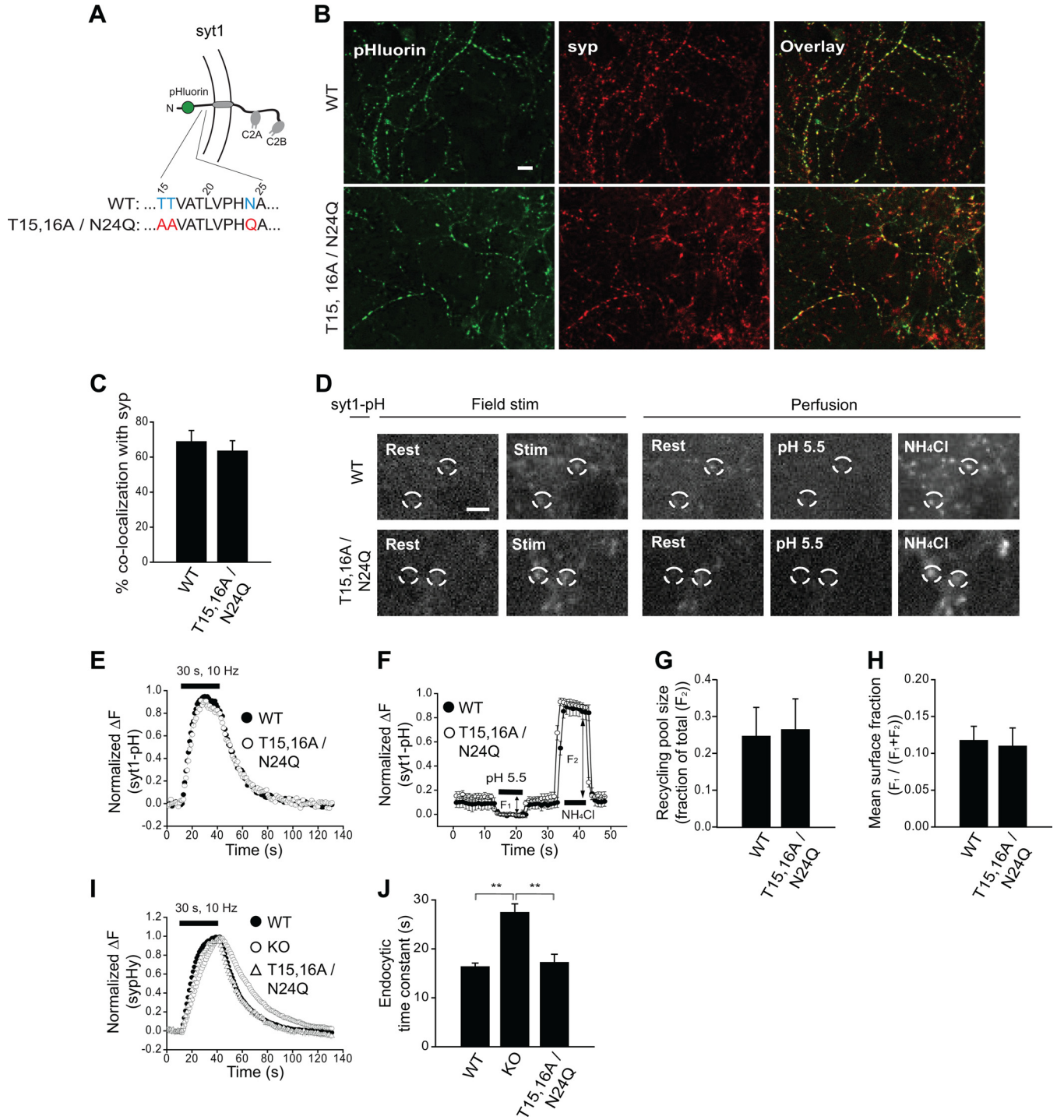

FIGURE 3. **Syt1 lacking all glycans is normally sorted to recycling SVs where it rescues normal rates of endocytosis.** *A*, schematic diagram shows glycosylated residues (*blue*) in WT syt1 that were disrupted via point mutations (*red*). *B*, immunocytochemistry of WT syt1-pH and mutant syt1-pH lacking all glycans (T15,16A/N24Q) expressed in syt1 KO neurons using lentivirus is shown. *Left*, an anti-GFP antibody was used to visualize syt1-pH. *Middle*, synapses were labeled using an anti-synaptophysin antibody (syp). *Right*, merged image is shown. *Scale bar*, 4 μm. *C*, quantification of results in *B* is shown. 68.7 $\pm$ 6.5% and 63.4 $\pm$ 6.0% of syp fluorescence co-localized with WT and T15,16A/N24Q mutant forms of syt1-pH, respectively. *D*, sample images from neurons expressing syt1-pH. *Top*, *first two panels* show boutons expressing WT Syt1-pH at rest and during a 10-Hz, 30-s stimulus train. The *next three panels* show the same boutons at rest, during perfusion with low pH buffer and during perfusion with the NH_4Cl buffer. *Bottom*, same experiments as described in the *top panel* were repeated using T15,16A/N24Q syt1-pH. *Scale bar*, 4 μm. *E*, average normalized fluorescence traces for WT (*closed circles*) and T15,16A/N24Q mutant forms (*open circles*) of syt1-pH in response to the 10-Hz, 30-s stimulus train are shown. Average is from four coverslips, 25 boutons each. *F*, average traces from the WT and mutant syt1 pHluorins are shown. The surface fluorescence signals were quenched by applying low pH solution (F_1). Internal acidic fluorescence signals were subsequently dequenched by NH_4Cl superfusion (F_2). Average is from four coverslips, 25 boutons each. *G*, recycling pool size was estimated by normalizing the magnitude of the evoked fluorescence change, 25 s after the beginning of the stimulus train (10 Hz, 30 s), to the size of the total acidified SV pool (F_2 as shown above). No significant difference was observed between WT and T15,16A/N24Q syt1-pHs. *H*, surface fraction of syt1-pH, which was estimated by $F_1/(F_1+F_2)$, was not significantly different between WT and T15,16A/N24Q syt1-pHs. *I*, SV cycling was assayed using sypHy in syt1 KO neurons expressing untagged WT or T15,16A/N24Q mutant syt1. The mutant form of syt1 rescued normal rates of endocytosis. Average is from three coverslips, 30 boutons each. *J*, average post-stimulus endocytic time constants from the experiments shown in *H* are displayed. **, $p < 0.01$. *Error bars*, S.E.

cycling using another optical reporter, pHluorin-tagged syp (sypHy). Compared with WT syt1, the glycosylation mutant completely rescued the slow endocytosis that was observed in syt1 KO neurons (WT: 16.3 ± 0.8 s; KO: 27.4 ± 1.8 s; T15,16A/N24Q: 17.2 ± 1.7 s) (Fig. 3, *I* and *J*). These findings further confirm that glycosylation plays no discernible role in the sorting or the function of syt1. The assay used in this study does not have sufficient temporal resolution to resolve a potential kinetic difference between WT and the mutant during exocytosis, *i.e.* rising phase of sypHy response. Nevertheless, we demonstrated that deletion of a large N-terminal segment of syt1, including all the glycosylation sites, fully rescued the release kinetics when targeted to synapses by fusing it with growth-associated protein-43 or synaptophysin (30, 31).

The N-Glycans Are Partially Dispensable for Targeting and Trafficking of SV2A—Whereas glycosylation is not important for sorting of syt1 as shown above, it might play an important role in the targeting or recycling of other SV membranes proteins. To address this question, we turned to another SV glycoprotein, SV2A, using a pHluorin-tagged version of this protein (SV2A-pH) (18). Fig. 4*A* shows the three *N*-glycosylation sites on an intraluminal loop of SV2A and the corresponding point mutations that were made to disrupt glycosylation (each mutation is designated as N1Q, N2Q, or N3Q). Below, we analyzed all the single and double point mutations of these glycosylation sites.

Because hippocampal neurons express SV2A and B, we used neurons derived from SV2A/B double KO mice as our model system. WT SV2A-pH, expressed in SV2A/B double KO neurons using lentivirus, was localized to synapses that were identified using an anti-synaptophysin antibody (Fig. 4*B*). Single point mutations in SV2A-pH (N1Q, N2Q, and N3Q), had no discernible effect on synaptic localization, consistent with a previous study (Fig. 4*C*) (15). Among the double point mutations, N2Q/N3Q and N1Q/N3Q resulted in the accumulation of SV2 in the cell body whereas the N1Q/N2Q mutation was tolerated (Fig. 4, *B* and *C*).

To test whether glycosylation is important for recycling of SV2A, neurons expressing WT or mutant forms of SV2A-pH (N1Q, N2Q, N3Q, and N1Q/N2Q) were depolarized using a 10-Hz, 30-s stimulus train, and the fluorescence changes at presynaptic boutons were monitored (Fig. 5*A*, *left panels*). Mutant forms of SV2A-pH that showed normal synaptic localization (N1Q, N2Q, N3Q, and N1Q/N2Q) behaved like the WT protein with a similar time course of recycling in response to the stimulus. In contrast, the N2Q/N3Q mutant accumulated in the soma and failed to respond to the stimulus, confirming that the protein failed to target recycling vesicles (Fig. 5*A*); the same trend was observed for the N1Q/N3Q mutant (data not shown). Average normalized traces from N1Q/N2Q and WT SV2A-pH are shown for comparison in Fig. 5*B*. The time courses for internalization after stimulation were not significantly different between WT SV2A-pH (WT: 17.2 ± 0.9 s) and the synaptically targeted mutant forms (N1Q: 17.8 ± 0.9 s, N2Q: 17.1 ± 1.1 s, N3Q: 16.9 ± 0.9 s, N1Q/N2Q: 17.4 ± 1.2 s) (Fig. 5, *B* and *C*).

Next, we determined whether the steady-state distribution of SV2A was affected by glycosylation, as detailed above in our analysis of the syt1 mutants, by superfusing low pH and NH_4Cl buffer solutions (Fig. 5*A*, *right panels*). WT and single point mutant forms of SV2A-pH exhibited little fluorescence change in response to low pH perfusion, suggesting that the expressed proteins were specifically targeted to SVs and were absent from the plasma membrane (Fig. 5*A*). This is in stark contrast to other pHluorin-tagged SV membrane proteins (*e.g.* syt1, syp, and synaptobrevin), which accumulate at significant levels on the plasma membrane (syt1-pH: 12 ± 2%, Fig. 3*H*) (syp: ~8%, synaptobrevin: ~24%) (22, 32). Single point mutations (N1Q, N2Q, N3Q), or the N1Q/N2Q double mutation, did not affect the steady-state distribution of SV2A. In contrast, most of the N2Q/N3Q mutant form of SV2A-pH was localized to the plasma membrane of the soma, as shown by the large reduction in fluorescence in the presence of low pH buffer (Fig. 5*A*).

Single point mutations (N1Q, N2Q, and N3Q) do not affect the expression level of SV2A (15). Analysis of double point mutations has shown that N2Q/N3Q severely reduces the expression level of SV2A, suggesting that these two glycosylated residues are required for ER quality control.[4] Interestingly, whereas the N1Q/N2Q double mutation leads to modest reduction of SV2A expression (15), it has no measurable effect on recycling of the protein (Fig. 5, *B* and *C*). In summary, unlike syt1, *N*-glycosylation sites of SV2A are not entirely dispensable for the sorting of the protein to cycling SVs.

Glycosylation Is Essential for the Synaptic Localization of Synaptophysin—Syp has a single *N*-glycan on the first intraluminal loop (Asn-53) (Fig. 6*A*). As noted above, a mutant form of syp, lacking the *N*-glycan, exhibited sorting to small translucent vesicles in human hepatoma cells, but the role of this modification in trafficking in neurons has not been addressed (19). We tested the effect of N53Q mutation in sypHy expressed in syp KO neurons. Immunostaining with an anti-GFP antibody revealed co-localization of WT sypHy with a synaptic vesicle marker, SV2A, consistent with the previous study (Fig. 6, *B* and *C*) (23). Unlike syt1-pH and SV2A-pH, in which the removal of single glycans was tolerated, the N53Q mutation in sypHy led to accumulation of the protein in the cell body of neurons (Fig. 6*B*), in sharp contrast to the lack of effect of this mutation in human hepatoma cells (19). We next analyzed the recycling of WT and N53Q mutant sypHy in response to a stimulus train (10 Hz, 30 s). WT sypHy showed a clear increase in fluorescence whereas N53Q sypHy, in the soma, did not respond at all (Fig. 6, *D* and *E*). We tested whether the impaired recycling of N53Q sypHy is because of reduced expression. Western blot analysis using anti-GFP antibody revealed that the expression level of sypHy was not altered by the N53Q mutation (Fig. 6*F*). These data clearly demonstrate that the lack of glycosylation severely affects targeting of syp to actively cycling SVs.

DISCUSSION

We have examined the localization and trafficking of glycosylation mutant syt1 proteins (both *N*- and *O*-) in syt1 KO

[4] M. Dong, personal communication.

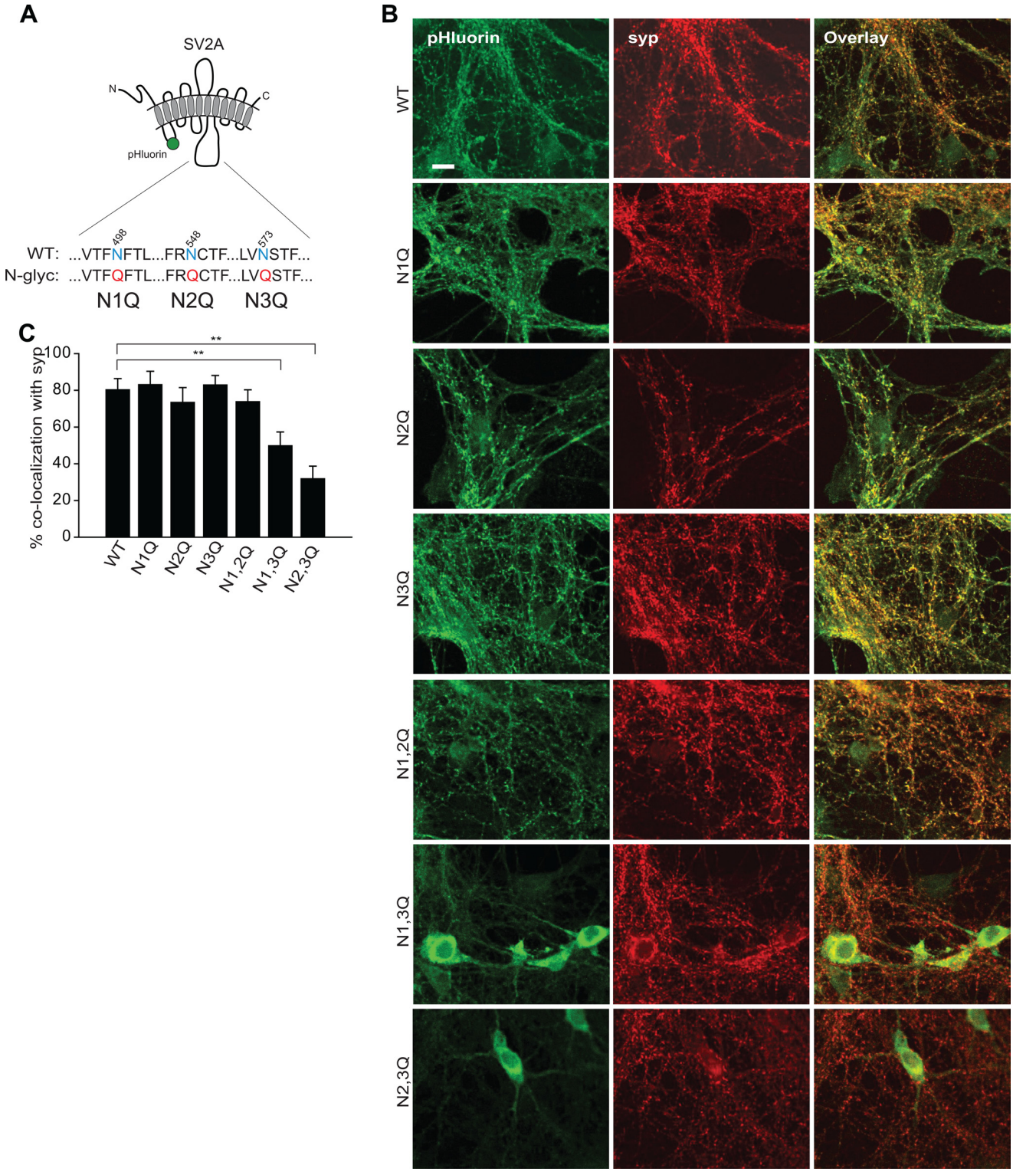

FIGURE 4. ***N*-Glycans on SV2A are partially dispensable for synaptic localization.** *A*, schematic diagram shows *N*-glycosylated residues (*blue*) in WT SV2A that were disrupted via point mutations (*red*). *B*, immunocytochemistry of WT and mutant forms of SV2A-pH expressed in SV2A double KO neurons is shown. An anti-GFP antibody was used to visualize SV2A-pH. Synapses were identified by staining with an anti-synaptophysin antibody. Of all proteins tested, only the N1Q/N3Q and the N2Q/N3Q double mutants accumulated in the cell body of neurons. *Scale bar*, 10 μm. *C*, quantification of the results in *B* is shown. The degree of co-localization of syp with each of the WT and mutant forms of SV2A-pH was as follows (in %): 80.3 $\pm$ 6.1 (WT), 83.1 $\pm$ 7.3 (N1Q), 73.4 $\pm$ 8.1 (N2Q), 82.9 $\pm$ 5.2 (N3Q), 73.8 $\pm$ 6.5 (N1Q/N2Q), 49.8 $\pm$ 7.5 (N1Q/N3Q), and 31.8 $\pm$ 6.9 (N2Q/N3Q). **, $p < 0.01$. *Error bars*, S.E.

neurons. In contrast to previous studies in neuroendocrine cells, we found that the glycosylation plays no measureable role in the sorting of syt1 to recycling SVs. Moreover, the nonglycosylated form of syt1 was able to rescue the slow endocytosis defect manifest in syt1 KO neurons, confirming that this mutant form of syt1 retained normal endocytic

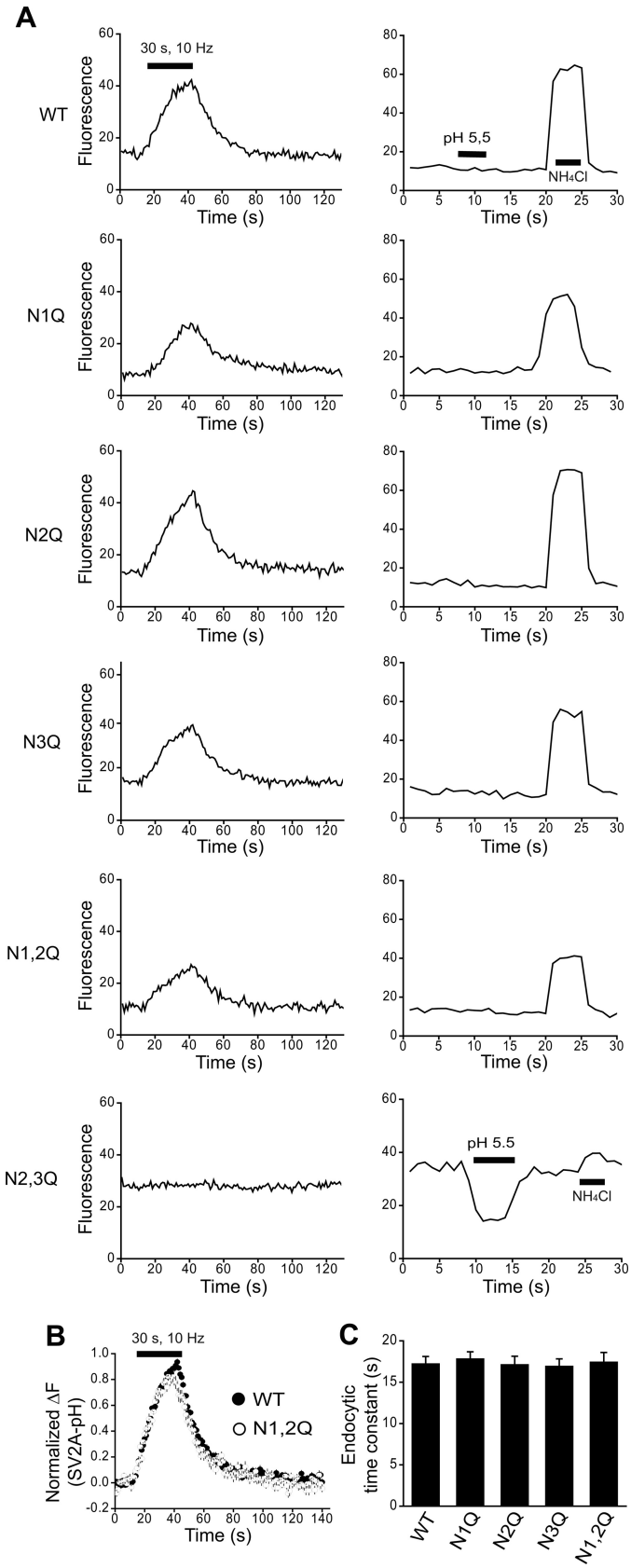

FIGURE 5. **Glycosylation regulates the trafficking and vesicular targeting of SV2A.** *A*, representative traces of WT and glycosylation mutant forms of SV2A-pH (*left*) show fluorescence changes in response to the 10-Hz, 30-s stimulus train and (*right*) the steady-state fluorescence distribution during perfusion with low pH (5.5) and NH_4Cl buffers. *B*, normalized average traces of fluorescence change, evoked by stimulus train (10 Hz, 30 s), from WT (*closed circles*) and N1/2Q mutant (*open circles*) forms of SV2A-pH are shown. Average is from three coverslips, 30 boutons each. *C*, comparison of endocytic time constants between WT and the mutant forms of SV2A-pH is shown. Average is from three coverslips, 30 boutons each. *Error bars*, S.E.

function. We showed previously that the plasma membrane-targeted C2AB domain of syt1, which lacks all glycosylation sites, fully rescued the release kinetics in syt1 KO neurons, suggesting glycosylation is not required for the exocytic function of the protein, either (30). An interesting finding in this study is that the fraction of plasma membrane-stranded syt1 can vary depending on the endogenous level of syt1, which suggests that there is competition between endogenous and transfected syt1 for a limited number of slots in each SV. It would be interesting to test whether similar trends are observed for other SV membrane proteins.

We also determined whether glycosylation sites on the other major glycoproteins of SVs, SV2A and syp, were important for sorting or recycling on SVs. The N1Q/N2Q mutant form of SV2A-pH exhibited unaltered targeting and recycling as compared with WT. In contrast, the N2Q/N3Q and N1Q/N3Q mutants accumulated in the cell body. These data suggest that the presence of the glycan on Asn-573, but not on Asn-498 or Asn-548 alone, is sufficient for vesicular sorting (Figs. 4 and 5). Thus, a specific subset of the *N*-glycans on SV2A functions in the sorting and targeting of this protein. These results have important implications for the role of individual glycans in mediating the entry of botulinum neurotoxins. It was reported previously that the glycan at Asn-573 is necessary and sufficient for entry of botulinum neurotoxin E into neurons whereas Asn-498 and Asn-548 are not required (15). It remained unclear as to whether loss of entry was because of impaired binding of the toxin to SV2A or defective endocytosis of the SV2A. The latter possibility can now be excluded as N573Q does not affect recycling of SV2A.

In the case of syp, the effect of the N53Q mutation was so dramatic that no detectable levels of the protein made it to synapses; we tested the recycling of N53Q syp in the soma in response to stimulus and saw no signal at all (Fig. 6). At present, the mechanism by which *N*-glycosylation regulates the vesicular targeting of syp and SV2A is unknown. *N*-Glycosylation might play indirect roles in vesicular targeting because this modification is generally important for the steps that precede the sorting of proteins into axonal compartments, such as protein folding and quality control in the ER. For syp, because an earlier study showed that the nonglycosylated mutant protein was sorted to small translucent vesicles in human hepatoma cells, glycosylation was thought to affect a step downstream from quality control in the ER (19). The fact that *N*-glycosylation is likely to be required for exit of syp from the ER in neurons indicates that different mechanisms of quality control might operate in neurons *versus* nonneuronal cells. Alternatively, the *N*-glycans might act directly as vesicular-targeting signals. This possibility was postulated by studies in polarized epithelial cells. In these cells, *N*- and *O*-glycans are recognized by specific lectins (*e.g.*

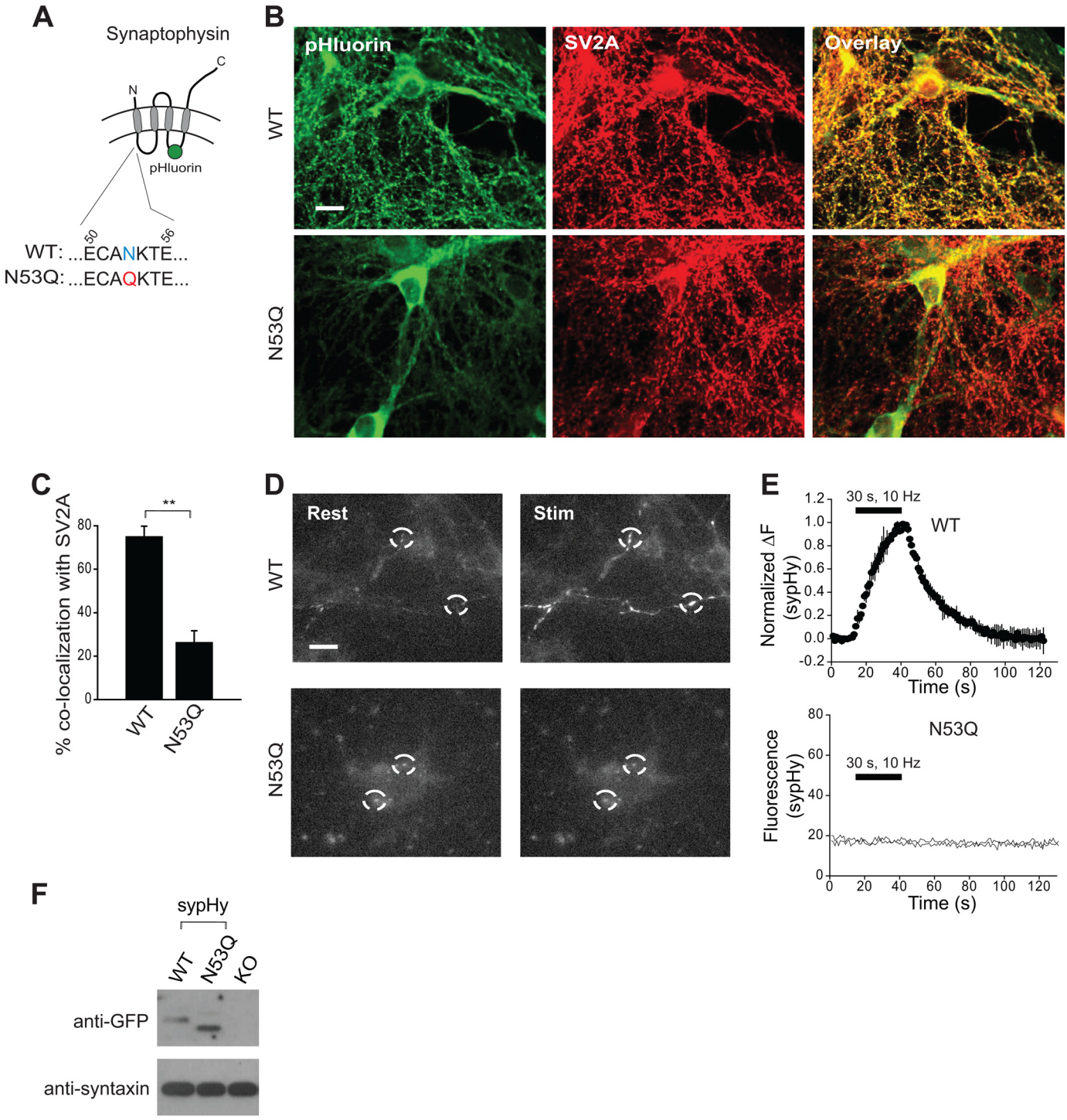

FIGURE 6. **Glycosylation affects the synaptic localization of syp.** *A*, schematic diagram shows the lone glycosylation site (*blue*) of syp; the N53Q point mutation is indicated in *red*. *B*, images from syp KO neurons, expressing WT or the *N*-glycosylation mutant form of sypHy are shown. An anti-GFP antibody was used to visualize sypHy; synapses were identified by staining with an anti-SV2A antibody. Whereas WT sypHy was localized to synapses, the N53Q mutant accumulated in the cell body. *Scale bar*, 15 μm. *C*, quantification of results in *B* is shown. 74.9 $\pm$ 4.9% and 26.2 $\pm$ 5.5% of SV2A fluorescence co-localized with WT and N53Q mutant forms of sypHy, are shown, respectively. *D*, syp KO neurons expressing WT or N53Q sypHy were depolarized using a 10-Hz, 30-s stimulus train. WT sypHy exhibited stimulus-induced changes in fluorescence whereas the N53Q mutant did not respond. Shown are representative examples (three coverslips, 30 boutons each). *Scale bar*, 5 μm. *E*, *top*, normalized average traces of fluorescence change, evoked by stimulus train (10 Hz, 30 s), from WT sypHy are shown. *Bottom*, N53Q mutant forms of sypHy show no fluorescence changes in response to the 10-Hz, 30-s stimulus train. *F*, Western blot shows expression levels of the WT and N53Q mutant forms of sypHy. Samples were prepared from syp KO neurons infected with lentivirus. Syntaxin served as a loading control. **, $p < 0.01$. *Error bars*, S.E.

galectin-3) in the lumen of the trans-Golgi network where sorting of glycosylated proteins to the apical membrane takes place (7). Whether such interaction between glycans and lectins occurs in neurons is not known; our results revealed that, if operative, such a mechanism would not apply to all SV proteins.

Acknowledgments—We thank M. B. Jackson, A. Audhya, and the Chapman laboratory for comments on this manuscript.

REFERENCES

1. Bonanomi, D., Benfenati, F., and Valtorta, F. (2006) Protein sorting in the synaptic vesicle life cycle. *Prog. Neurobiol.* **80,** 177–217
2. Hannah, M. J., Schmidt, A. A., and Huttner, W. B. (1999) Synaptic vesicle biogenesis. *Annu. Rev. Cell Dev. Biol.* **15,** 733–798
3. Sampo, B., Kaech, S., Kunz, S., and Banker, G. (2003) Two distinct mechanisms target membrane proteins to the axonal surface. *Neuron* **37,** 611–624
4. Kittler, J. T., and Moss, S. J. (2003) Modulation of $GABA_A$ receptor activity by phosphorylation and receptor trafficking: implications for the efficacy of synaptic inhibition. *Curr. Opin. Neurobiol.* **13,** 341–347
5. Haas, K. F., and Broadie, K. (2008) Roles of ubiquitination at the synapse. *Biochim. Biophys. Acta* **1779,** 495–506
6. Vagin, O., Kraut, J. A., and Sachs, G. (2009) Role of *N*-glycosylation in trafficking of apical membrane proteins in epithelia. *Am. J. Physiol. Renal Physiol.* **296,** F459–469
7. Duffield, A., Caplan, M. J., and Muth, T. R. (2008) Protein trafficking in polarized cells. *Int. Rev. Cell Mol. Biol.* **270,** 145–179
8. Takamori, S., Holt, M., Stenius, K., Lemke, E. A., Grønborg, M., Riedel, D., Urlaub, H., Schenck, S., Brügger, B., Ringler, P., Müller, S. A., Rammner, B., Gräter, F., Hub, J. S., De Groot, B. L., Mieskes, G., Moriyama, Y., Klingauf, J., Grubmüller, H., Heuser, J., Wieland, F., and Jahn, R. (2006) Molecular anatomy of a trafficking organelle. *Cell* **127,** 831–846
9. Nishiki, T., and Augustine, G. J. (2004) Synaptotagmin 1 synchronizes transmitter release in mouse hippocampal neurons. *J. Neurosci.* **24,** 6127–6132
10. Geppert, M., Goda, Y., Hammer, R. E., Li, C., Rosahl, T. W., Stevens, C. F., and Südhof, T. C. (1994) Synaptotagmin 1: a major Ca^{2+} sensor for transmitter release at a central synapse. *Cell* **79,** 717–727
11. Han, W., Rhee, J. S., Maximov, A., Lao, Y., Mashimo, T., Rosenmund, C., and Südhof, T. C. (2004) *N*-Glycosylation is essential for vesicular targeting of synaptotagmin 1. *Neuron* **41,** 85–99
12. Kanno, E., and Fukuda, M. (2008) Increased plasma membrane localization of *O*-glycosylation-deficient mutant of synaptotagmin 1 in PC12 cells. *J. Neurosci. Res.* **86,** 1036–1043
13. Janz, R., and Südhof, T. C. (1999) SV2C is a synaptic vesicle protein with an unusually restricted localization: anatomy of a synaptic vesicle protein family. *Neuroscience* **94,** 1279–1290
14. Chang, W. P., and Südhof, T. C. (2009) SV2 renders primed synaptic vesicles competent for Ca^{2+}-induced exocytosis. *J. Neurosci.* **29,** 883–897
15. Dong, M., Liu, H., Tepp, W. H., Johnson, E. A., Janz, R., and Chapman, E. R. (2008) Glycosylated SV2A and SV2B mediate the entry of botulinum neurotoxin E into neurons. *Mol. Biol. Cell* **19,** 5226–5237
16. Nowack, A., Yao, J., Custer, K. L., and Bajjalieh, S. M. (2010) SV2 regulates neurotransmitter release via multiple mechanisms. *Am. J. Physiol. Cell Physiol.* **299,** C960–967
17. Daly, C., Sugimori, M., Moreira, J. E., Ziff, E. B., and Llinás, R. (2000) Synaptophysin regulates clathrin-independent endocytosis of synaptic vesicles. *Proc. Natl. Acad. Sci. U.S.A.* **97,** 6120–6125
18. Kwon, S. E., and Chapman, E. R. (2011) Synaptophysin regulates the kinetics of synaptic vesicle endocytosis in central neurons. *Neuron* **70,** 847–854
19. Leube, R. E., Wiedenmann, B., and Franke, W. W. (1989) Topogenesis and sorting of synaptophysin: synthesis of a synaptic vesicle protein from a gene transfected into nonneuroendocrine cells. *Cell* **59,** 433–446
20. Eshkind, L. G., and Leube, R. E. (1995) Mice lacking synaptophysin reproduce and form typical synaptic vesicles. *Cell Tissue Res.* **282,** 423–433
21. Janz, R., Goda, Y., Geppert, M., Missler, M., and Südhof, T. C. (1999) SV2A and SV2B function as redundant Ca^{2+} regulators in neurotransmitter release. *Neuron* **24,** 1003–1016
22. Fernández-Alfonso, T., Kwan, R., and Ryan, T. A. (2006) Synaptic vesicles interchange their membrane proteins with a large surface reservoir during recycling. *Neuron* **51,** 179–186
23. Granseth, B., Odermatt, B., Royle, S. J., and Lagnado, L. (2006) Clathrin-mediated endocytosis is the dominant mechanism of vesicle retrieval at hippocampal synapses. *Neuron* **51,** 773–786
24. Miesenböck, G., De Angelis, D. A., and Rothman, J. E. (1998) Visualizing secretion and synaptic transmission with pH-sensitive green fluorescent proteins. *Nature* **394,** 192–195
25. Liu, H., Dean, C., Arthur, C. P., Dong, M., and Chapman, E. R. (2009) Autapses and networks of hippocampal neurons exhibit distinct synaptic transmission phenotypes in the absence of synaptotagmin I. *J. Neurosci.* **29,** 7395–7403
26. Jiang, M., and Chen, G. (2006) High Ca^{2+}-phosphate transfection efficiency in low-density neuronal cultures. *Nat. Protoc.* **1,** 695–700
27. Dong, M., Yeh, F., Tepp, W. H., Dean, C., Johnson, E. A., Janz, R., and Chapman, E. R. (2006) SV2 is the protein receptor for botulinum neurotoxin A. *Science* **312,** 592–596
28. Dean, C., Liu, H., Dunning, F. M., Chang, P. Y., Jackson, M. B., and Chapman, E. R. (2009) Synaptotagmin 4 modulates synaptic function and long-term potentiation by regulating BDNF release. *Nat. Neurosci.* **12,** 767–776
29. Kanno, E., and Fukuda, M. (2007) Increased plasma membrane localization of *O*-glycosylation-deficient mutant of synaptotagmin 1 in PC12 cells. *J. Neurosci. Res.*
30. Yao, J., Kwon, S. E., Gaffaney, J. D., Dunning, F. M., and Chapman, E. R. (2012) Uncoupling the roles of synaptotagmin 1 during endo- and exocytosis of synaptic vesicles. *Nat. Neurosci.* **15,** 243–249
31. Hui, E., Johnson, C. P., Yao, J., Dunning, F. M., and Chapman, E. R. (2009) Synaptotagmin-mediated bending of the target membrane is a critical step in Ca^{2+}-regulated fusion. *Cell* **138,** 709–721
32. Wienisch, M., and Klingauf, J. (2006) Vesicular proteins exocytosed and subsequently retrieved by compensatory endocytosis are nonidentical. *Nat. Neurosci.* **9,** 1019–1027